Optically Detected Magnetic Resonance; Computational Predictions and Experimental Results

Scott Leland Crossen

A senior thesis submitted to the faculty of
Brigham Young University
in partial fulfillment of the requirements for the degree of

Bachelor of Science

Dr. John S. Colton, Advisor

Department of Physics and Astronomy

Brigham Young University

[Approval Month] [Year]

ABSTRACT

Optically Detected Magnetic Resonance; Computational Predictions
and Experimental Results

Scott Leland Crossen
Department of Physics and Astronomy, BYU
Bachelor of Science

[The abstract is a summary of the thesis/dissertation with emphasis on the findings of the study. The abstract must not exceed 350 words in length and fit on one page, single spaced.]

Keywords: [A comma-separated list of descriptive words for search purposes]

Contents

Table of Contents iii

List of Figures 1

1 Introduction 3
- 1.1 Qualitative Description of ESR and ODMR . . . 3
- 1.2 The Defect Nature of Materials . . . 5
- 1.3 Electron Spin, Quantum Computing, and Qubits . . . 6
- 1.4 Previous Work (Our Research Group and Others) . . . 8
  - 1.4.1 Preliminary Work and Results . . . 8
  - 1.4.2 Experimental Setup . . . 9
  - 1.4.3 Samples and Collaborative Efforts . . . 9
  - 1.4.4 EasySpin Computational Modeling System . . . 10
- 1.5 Preliminary Results of Experimental ODMR . . . 10
- 1.6 Overview of Thesis . . . 11
- 1.7 Explanatory Notes and Background Information . . . 13

2 Computational Model and Theory 15
- 2.1 Mathematical Theory . . . 15
- 2.2 EasySpin Interaction Modeling System . . . 16
  - 2.2.1 The EasySpin Struct Definition . . . 17
  - 2.2.2 Basic Class Structure . . . 17
- 2.3 Selecting Hamiltonian Arguments . . . 19
  - 2.3.1 ZnO Nanowires . . . 19
  - 2.3.2 Irradiated 4H-SiC . . . 20
  - 2.3.3 Thin-Film CdTe . . . 21

3 Experimental Methods 22
- 3.1 Preparation of Silicon Carbide Samples . . . 22
- 3.2 Preparation of Cadmium Telluride Samples . . . 22
- 3.3 Experiment Background . . . 22
- 3.4 Experiment Setup . . . 22

3.5 Data processing 22

4 Results **23**
4.1 Computational Predictions 23
4.2 Experimental Results 23
4.3 Data Analysis 23
4.4 Conclusion 23

Appendix A Electron Spin Studies of Electron Irradiated SiC **25**

Appendix B Optical Studies of Cadmium Telluride **26**

Appendix C Electron Spin Coherence of Silicon Vacancies in Proton-Irradiated 4H-SiC **27**

Bibliography **28**

List of Figures

1.1 Zeeman effect and resonant conditions in matter 5

1.2 Magnetic field and microwave frequency relationship 11

1.3 Preliminary ODMR data 12

2.1 Simple Spin System Definition 17

2.2 Example of spin-hamiltonion fields 19

2.3 ESR Spectrum Presented by Stehr et al. 19

2.4 Recreation of ZnO Nanowire ESR 20

2.5 The *EasySpin* representation of SiC 21

2.6 The *EasySpin* representation of CdTe 21

3.1 SiC energy levels and zero-field splitting 22

4.1 ODMR computational model for SiC 23

4.2 ODMR computational model for CdTe 23

4.3 Experimental ODMR for SiC 24

4.4 Experimental ODMR for CdTe 24

A.1 Electron-irradiated SiC lifetime summary 25

A.2 ODMR/Photoluminescence vs temperature 25

B.1 Photoluminescence of CdTe 26

4.1 Setup for using counter-propagating light 27

Chapter 1

Introduction

1.1 Qualitative Description of ESR and ODMR

Optically Detected Magnetic Resonance (ODMR) is a particular form of *Electron Paramagnetic Resonance* (EPR) which is more commonly known as *Electron Spin Resonance* (ESR). The latter two of these terms (EPR and ESR) are synonymous; The former (ODMR) is a particular subset of ESR that utilizes a luminescence measuring technique as a means to collect ESR information. In literature, it is common to see both of these terms followed by the designation "spectroscopy" which signifies that they are tools to study properties of matter via electromagnetic radiation. Though the extent of their application has grown over the years, ESR and ODMR are most commonly used to study the spin-properties of electrons and electron-holes trapped in metal lattices. They can be used to study free radicals in organic materials and are also important in studying the local environment of lattice defects through a technique using angular-dependent ODMR. One particular use of ODMR is the study of electron-spin coherence via a technique known as *Electron Spin Echo*. This can be useful when studying what properties and conditions lead to superior state coherence for qubit candidate materials in quantum computing.

The intellectual foundation of Electron Spin Resonance is rooted in Quantum Mechanics. Bound electrons in matter have discrete and quantized energy levels that govern what frequencies of light are emitted when transitions between energy levels are made. For electron systems, which are fermions and thus subject to the Pauli exclusion principle, the energy levels are 2nd order degenerate when bound in matter. In Quantum Mechanics we choose to describe this degeneracy in terms of spins: we say an electron is either "spin-up" or "spin-down". Each energy level can have at most two electrons of opposite spins inhabiting it (and thus the degeneracy). The spin terminology is arbitrary however, and is really just an attempt at comparing electrons to particles. In truth, electron spin is a term for a property that is emergent from solving the wave equation. However, it nonetheless describes the principle of conservation of momentum that would be found in classical system such as a top and so the term makes sense and has persisted in usage today. In this case, the electron's spin is a description of the magnetic moment for when the particle is in the presence of a magnetic field. In the case of electrons bound in matter within a magnetic field, the energy levels of the molecule will split according to the "Zeeman Effect" and the spin-states of the electrons can be observed - most commonly through a photoluminescence or other fluorescence measuring technique.

The Zeeman effect itself is crucial in understanding the principles of ESR. In the presence of a magnetic field, populations of free electrons will form a spin-1/2 system between a higher-energy "spin-up" state and a lower-energy "spin-down" state. In matter, different parities of spin-states can be formed between the interactions of different energy levels with different transition selection rules. A spin-1/2 system in the presence of a magnetic field is shown in 1.1. As seen here, the energy levels of the two differing spins diverge linearly for an increasing magnetic field. The difference in energy between these two levels is typically in the microwave frequency domain. For a given magnetic-field strength there will be a set of characteristic microwave frequencies that the electrons are most prone to emitting when transitioning between these quantized states. In

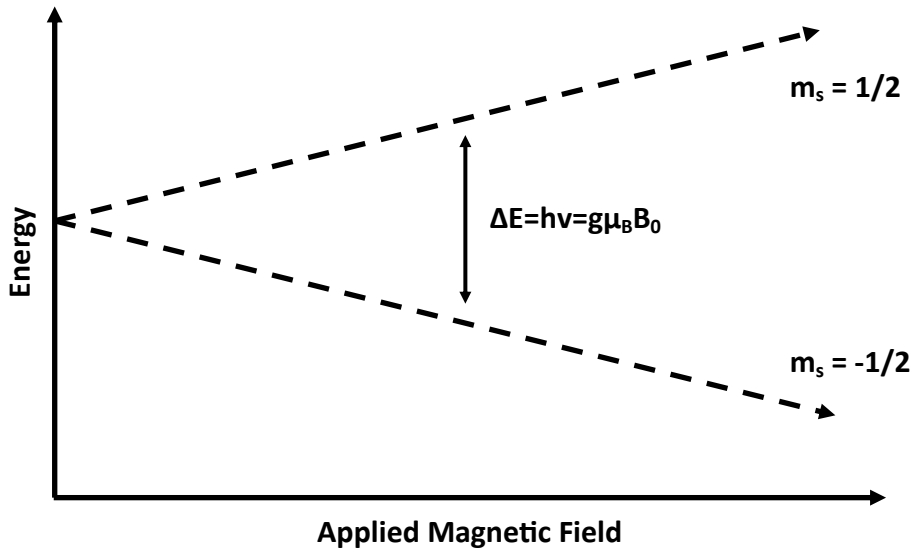

Figure 1.1 Zeeman effect for a two level system showing spin ($\pm 1/2$) energy levels as a function of applied magnetic field. For arbitrary field strength the energy difference is shown as a function of μ, g, and the field strength B.

a spin-1/2 system there will only be one frequency for a given magnetic field corresponding to the difference between the two zeeman lines at the given field strength. Likewise, for a given microwave target signal, there will be a variety of magnetic field strengths which are most adept at transitioning bound electrons between states. This unique pairing between both the microwave frequency and magnetic field strength is the resonant condition upon which ESR is based off of and also the means it uses to discover information about materials.

1.2 The Defect Nature of Materials

[Rough - More] In solid-state physics, materials form crystal lattices for molecular tessellation. These structures are not perfect, however, and often have intrinsic interstitial defects. These defects come in the form of either additional or missing atoms. [continued]

[Rough - More] Crystal lattice defects are important as they contribute to the overall spin

system of the material via either electrons or electron-holes.

[Rough - More] Optically Detected Magnetic Resonance (ODMR) can be used in conjunction with a varied applied angle (between the magnetic field and c-plane) to study the local nature of each type of defect in the material.

[Rough - More] ODMR can give the information necessary in understanding how the lattice is formed.

[Rough - More] Defects can be introduced via high-fluence irradiation of particles.

1.3 Electron Spin, Quantum Computing, and Qubits

Classical Computation is almost always based upon a binary system. In these architectures, the computer's register, memory, and general logical states are either in a logical 'true' or a logical 'false' state. A 'true' state corresponds to a high voltage and a 'false' state corresponds to a grounded voltage. A computer's bits can be in either of these two states - 1 or 0 - but not both.

A spin-1/2 system also describes a binary system between a higher-energy basis state and a lower-energy basis state. In this comparison, the spin-1/2 system will be measured (and the wave function collapsed) to be in either of these two states - but not both. The important difference between the the spin-1/2 system and the classical computer bit model is that the spin system can have states that exist as linear combinations of the two basis up/down states. In accordance with Quantum Mechanics, this means that the spin-1/2 system can exist as a superposition between both the spin-up and spin-down states and has a certain probability of being measured in each. It is important to note that this superposition does not mean that the state exists as some value in between an excited state and a lower state. Rather, it exists with some value in both states simultaneously.

Because of this unique property of spin systems, they can be used as a basis for forming what is

called a "quantum computer". Though it largely depends on the architecture, Quantum computers can be thought of to manipulate information in a similar fashion to that of a classical computer. Both have logical operators and storage bits and both are algorithmically based. Quantum computers, however, utilize this unique possibility of superposition to make probabilistic calculations for many different states at the same time. This happens through the quantum mechanical operators that initialize and manipulate the states that are stored in "qubits" - or the quantum computer's version of classical bits that can exist in these superposition types of states. Because of the existing theoretical construction from nondeterministic finite automata to deterministic finite automata, quantum computers are also "turing complete" in the broad definition of that term. This statement is trivial however, because quantum computers can be operated in the discrete binary limit and so should be able to do anything a classical computer can.

Today, there is large emphasis within the scientific community in building viable, scalable quantum computers. The reason for this is that quantum computers offer reduced computational time limits for certain types of algorithms. Certainly however, these machines are not necessarily more adept at common tasks such as processing videos to be scrubbed by common users, but are rather designed to carry out a few types of intense calculations in logarithmic time that would normally have a polynomial time dependence. The most notable use for quantum computers in our modern society is within the field of computer security and encryption. Quantum computers have the ability to compute prime factors via Shor's algorithm in a much faster time than traditional computers. This ability would essentially render all of the current RSA encryption methods obsolete in addition to anything that relies on public/private key encryption such as bitcoin.

Although more than just spin systems can be used as the all-important qubits for quantum computing, we will focus on this type - specifically spin-1/2 systems formed from electrons - for the basis of our discussion. As mentioned earlier, Electron Spin Resonance is the major tool used to study the spin properties of materials. In the case of quantum computation, ESR is used to study

possible qubit materials that might eventually be used in such machines. Currently, one of the major difficulties in creating quantum computers is finding materials that can form superposition states that remain coherent (and reliable) over prolonged periods of time. In order to understand what properties of materials lead to superior qubit construction and state coherence, ESR can be used in conjunction with electron spin echo experiments to study the coherence of electrons in a spin-1/2 system. Moreover, ESR can be used alone to study the spin system itself and the local environment of the defects in materials that form them. Knowledge of this important topic will serve to increase our ability to construct better qubits for use in quantum computers.

1.4 Previous Work (Our Research Group and Others)

1.4.1 Preliminary Work and Results

The work performed in this thesis references in large part the work done by Kyle Miller and Jacob Embley - two students who worked under Dr. John Colton and have since graduated from Brigham Young University. Their work was mostly performed on the topic of Electron Spin Coherence in Proton-Irradiated Silicon Carbide and is documented in their senior theses both of related titles. This thesis, however, will not be on the same topic as the former two but will expand on one aspect used by both of these two students in their work - ODMR. In addition, both Miller and Embley used a particular species of SiC which is one of the two principal materials of investigation in this thesis.

Appendix C includes a publication that Embley, Colton, Miller, Myself and a few others produced on the topic of spin coherence in proton irradiated silicon carbide. It has been accepted by *Physical Review B* and will appear in publication later in the year 2017. This publication serves as a capstone to the work of both Embley and Miller as included in their senior theses and will serve as the context for which this thesis was produced.

In addition to the work done by Miller and Embley, an additional study was performed on a similar material of the SiC specimen which is not included in either the aforementioned theses or publication. This project is included in Appendix A. The major difference with Appendix A and the theses produced by Miller and Embley is the fluence of irradiation used on the SiC sample in question. Miller's work was primarily concerned with a 10^{14} cm^{-2} proton-irradiated sample of SiC. Embley likewise worked with a 10^{13} cm^{-2} proton-irradiated sample of SiC. In Appendix A I work with a 10^{17} cm^{-2} electron-irradiated sample of SiC in much the same way as used by Embley. With this additional sample, a more comprehensive analysis and additional results are presented.

1.4.2 Experimental Setup

The experimental setup used for the majority of this thesis was set up and tested by Kyle Miller and Jacob Embley. Miller initially set up all the necessary instrumentation to be used in his experiment which is detailed in his thesis. Later, Embley improved upon most of Miller's design and achieved increased precision and improved results. The experiment used by both Embley and Miller was eventually repurposed and slightly modified for the experiment detailed in this thesis. A full summary and implementation of the experimental setup can be found in 3.4. This section includes both the setup used by Miller and Embley as well as the components I modified for the purposes of performing this work.

1.4.3 Samples and Collaborative Efforts

The work done for this thesis was done in collaboration with two groups of people. Firstly, the silicon carbide samples used were produced and partially characterized by Dr. Sam Carter of the Naval Research Lab. These samples were irradiated with different fluences of particles in order to introduce different concentrations of defects into the material. It was Carter's work that ultimately led us to obtain such high quality samples for optical characterization and electron spin resonance

studies.

The second collaborative group that we worked with was Dr. Mike Scarpulla of the University of Utah. Scarpulla was responsible for providing the second species of material (CdTe) that was characterized for this report. Like the SiC, this sample was provided with partial characterization and given to us for optical study. Appendix B gives the full report (at least up to the publication date of this thesis) for the optical studies performed on the CdTe sample.

1.4.4 EasySpin Computational Modeling System

EasySpin is a library for MATLAB designed to computationally model ESR data. The majority of computational work for this thesis was done using this program which was provided free of charge by the vendor's website. Though most of the necessary functions to model ESR data were included in the EasySpin library, I still found it necessary to create custom definitions in addition to what was already supplied.

1.5 Preliminary Results of Experimental ODMR

The work done for this thesis is based around two different materials. The first, SiC, has had prior work done on it for ODMR characterization. The second sample, CdTe, was not optically characterized for this work prior to our experimentation and was left to us for detailed analysis.

[Rough] Dr. Sam Carter of the Naval Research Lab provided the samples for the silicon carbide used. In addition, he also presented a series of plots to describe the spin system present in the material. According to the information he provided, the silicon vacancies in silicon carbide form a spin-3/2 system with a metastable doublet state to allow for non-radiative transitions. Another interesting characteristic of this system is that it has a zero-field splitting effect which accounts for a difference of energies without a magnetic field between the spin states +1/2 and +3/2 with -1/2

Figure 1.2 The relationship between magnetic field strength and microwave Frequency for 4H-SiC, a spin-3/2 system. Resonant conditions are shown via bright coloration on the axes of frequency vs field. Notice the linear dependence between both microwave energy and field strength.

and -3/2.

In addition to the information provided by Dr. Carter regarding the spin system of SiC, he also provided preliminary ODMR results performed at low field strengths of around 31 mT. The results of his measurements are found in 1.3 and show the transitions between different spin states which will be more fully developed in 3.1. Moreover, Carter also provided angular dependent measurements of the resonant relationship between magnetic field strength and microwave frequency. As mentioned in 1.1, there exists a unique pairing between the applied magnetic field and the resonant microwave energy transition. For a given magnetic field there will exist different resonant frequencies depending on the spin system in question. In addition, these characteristic frequencies will have associated linewidths that describe what range of frequencies the gaussian distribution is centered around and how wide it is. For the case of a spin-3/2 system as found in 4H-SiC, the relationship is best represented by 1.2 which is a plot produced by Dr. Carter for the samples used in this project.

1.6 Overview of Thesis

The purpose of this thesis is to describe in detail the methods and procedures behind experimental and theoretical ESR and to answer the question as to how both experimental and theoretical methods compare to each other. By so doing we will also introduce the fundamental theory behind ESR and computational modelling packages such as *EasySpin*. In addition, we will also discuss the experimental frameworks and setups necessary for collecting ODMR information from materials. This analysis will not be comprehensive but is rather purposed as an introduction into the

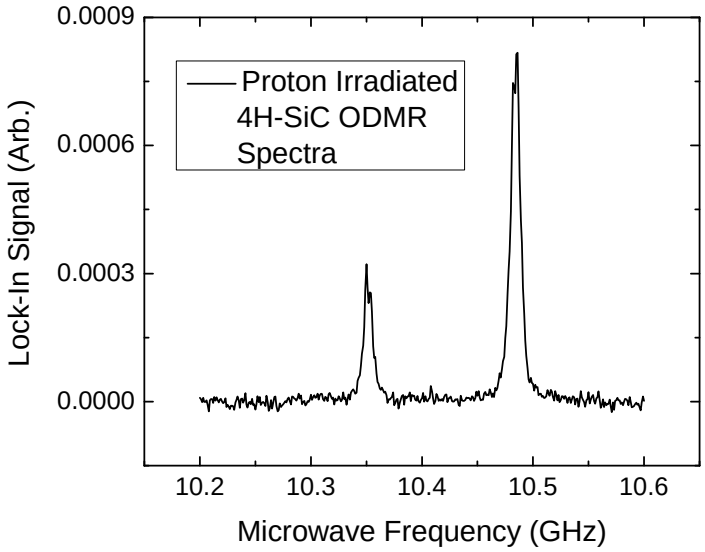

Figure 1.3 The preliminary ODMR data for Proton Irradiated Silicon Carbide in a constant magnetic field of 2.455 Tesla. The plot shows resonant paramagnetic conditions at 10.35 GHz and 10.47 GHz where the absorption is greatest.

techniques used in the field. As such, we will restrict our analysis to only solid-state ESR and ODMR.

In addition, this thesis will analyze what factors and properties inherent in materials contribute to ESR detection and spectroscopy. This analysis will be geared towards understanding the nature of defects within materials and how these defects are emergent in ODMR spectroscopy. As a final note on this topic we will introduce multiple examples of different defect-types to show resultant ODMR data.

We will use two main materials for this thesis: SiC and CdTe. These materials will be valuable in our understanding of lattice defect contribution towards ODMR results. In addition, we will primarily use these as controls to compare the experimental data with respective computational predictions. It will be through these two specimens that we will ultimately show the similarity between experimental results and theoretical predictions.

In the end, this thesis will conclude that computational modelling is accurate to the same degree as the spin system is understood. In other words: the level of precision that computational modelling can present is restricted by how much information is known about the hamiltonian for that given system.

As supplementary material, I have included multiple appendixes detailing further expansion projects and studies of ESR. Though these appendices are not purposed with the same thrust as this thesis, all of them are excellent resources that would serve to broaden the reader's understanding of the applications and use of this important experiment in condensed-matter physics.

1.7 Explanatory Notes and Background Information

The content of this thesis will use the term *ESR* when referring to the general theory and mathematical model of Electron Spin Resonance and will use the term *ODMR* when referring to the experimental methods used for collecting ESR information. As mentioned earlier, ODMR is a specific type of ESR that is ultimately used to collect the same information through a fluorescence technique. Because we have implemented an ODMR-type experiment in our lab we will use this term for descriptive accuracy when referring to our experimental application.

By way of information, the work done for this thesis was performed using MATLAB R2016b (version 9.1) and EasySpin version 5.1.9 . It will be assumed that the reader is proficient in basic MATLAB or C constructs and is at least familiar with data types and terms such as "struct", "parameter" and "field" as related to computer programming.

All plots and figures were created using a combination of Mathematica version 10.4 and Origin version 7.5.

In addition, pertinent git repositories will be hosted online via GitHub for all code developed for this project. The LabVIEW suite used for data acquisition can be found at the permanent

URL https://github.com/coltonlab/LabVIEW-programs. The programs developed on top of the EasySpin library that were used for theoretical modeling can be found along with this thesis at https://github.com/scottcrossen/SeniorThesis.

Chapter 2

Computational Model and Theory

2.1 Mathematical Theory

As mentioned in the introduction, Spin systems and Electron Spin Resonance are best understood in terms of interaction Hamiltonians. 'Hamiltonians' in this context are quantum mechanical operators (as opposed to the classical mechanical version) that act on energy states and form specific eigensystems with defined energy eigenvalues. For example, In the zeeman effect there exists a Hamiltonian that - when diagonlized - gives the energy-splitting for a given magnetic field in terms of it's eigensystem. Since ESR spectroscopy measures the resonant conditions between energy-levels and magnetic field strength, it is important to find the field-dependent Hamiltonian for each system before we can calculate the theoretical ESR spectrum.

[Rough] Thankfully, the general Hamiltonian for atoms in a magnetic field is commonly known. In this case, the interaction energy of an atom in a constant magnetic field is given by the overall spin Hamiltonian $\mathscr{H}_{tot}$:

$$\mathscr{H}_{tot} = \mathscr{H}_{elect} + \mathscr{H}_{cf} + \mathscr{H}_{LS} + \mathscr{H}_{SS} + \mathscr{H}_{Zee} + \mathscr{H}_{hfs} + \mathscr{H}_{Q} + \mathscr{H}_{N}$$

where $\mathscr{H}_{elect}$ is the electronic energy, $\mathscr{H}_{cf}$ is the crystal field energy, $\mathscr{H}_{LS} = \lambda L \cdot S$ is the spin-orbit

Figure 2.1 An Example of Spin-Hamiltonian fields in terms of S and g

interaction, $\mathscr{H}_{SS} = D\left[S_z^2 - \frac{1}{3}S(S+1)\right]$ is the spin-spin interaction, $\mathscr{H}_{Zee} = \beta H \cdot (L+2S)$ is the zeeman interaction energy, $\mathscr{H}_{hfs} = (A_x S_x I_x + A_y S_y I_y + A_z S_z I_z)$ is the hyperfine structure, $\mathscr{H}_Q$ is the quadrupole energy, and $\mathscr{H}_N = \gamma\beta_N H \cdot I$ is the nuclear spin energy. All of these component terms are defined in terms of the spin angular momentum operator S, the orbital angular momentum operator L, the Nuclear Spin Operator I, the Bohr magneton β, the spin-orbit coupling constant λ, the hyperfine coupling constant A, the nuclear gyrmagnetic ratio γ, and the zero-field splitting constant D.

Some terms in the Hamiltonian dominate the system and can be focused on individually. Though we will will not restrict our analysis to them, the most important terms are the zeeman interaction energy, the crystalline electric field, the spin-spin interaction energy, and the hyperfine term. We will specifically review all of these terms at some point in this paper.

[Rough - More] I should probably give a more in-depth explanation of the all-important zeeman term at this point. During this explanation I'll explain the g-tensor (and it's simplifications) and the spin parameter S.

[Rough] Once the Hamiltonian is known for the system, the ESR spectrum can be computationally predicted. A variety of methods are available to go from the basic Hamiltonian components to the finished ESR plot but the most notable is a software suite called *EasySpin* which vastly simplifies the amount of calculations and explicit Hamiltonian definitions that the user has to make.

2.2 EasySpin Interaction Modeling System

The purpose of this thesis is to comprehensively show the intricacies and unique methodologies of both computational and experimental ESR. As for the first of these two, the most common tool

Figure 2.2 An example declaration of the basic EasySpin struct used in defining the spin system.

used to computationally model ESR is known as *EasySpin*. This package is built as an open library on top of the MATLAB program and serves to add functionality to the already-useful suite of functions that MATLAB already consists of.

2.2.1 The EasySpin Struct Definition

The core utility to the EasySpin package is the struct definition for the spin system. The EasySpin library is built around the idea of a struct to define all necessary components of the system being studied. In fact, most methods in the EasySpin library usually only require a struct of this type as the sole parameter in the function declaration.

The struct represents the spin system and is usually defined by the user to the extent that the system is known. Though there are many optional parameters that can be included in the struct, the most simplest spin system needs to include a '.S' parameter representing either a list or a value for the parity of spin being worked with as well as a '.g' parameter to represent the g-factor of that material in solid-state ESR. The g-factor could be either a list or a value depending on the crystal type being investigated. After these two parameters are defined, the system can then be passed to any other functions for analysis and plotting. Figure 2.1 shows an example of what this basic definition might look like in MATLAB.

2.2.2 Basic Class Structure

The term 'class' is used loosely in this context. Unlike most languages, MATLAB (and thus EasySpin) is based on C and thus not really object oriented. However, unlike C, basic class definitions have been added to the program (but which still aren't commonly used). EasySpin uses a

Table 2.1 List of possible *EasySpin* plotting functions. '*pepper*' is the main function that will be used in this thesis.

Function	Description
garlic	cw EPR, isotropic and fast motion
chili	cw EPR, slow motion
pepper	cw EPR, solid state
salt	ENDOR, solid state
saffron	pulse EPR/ENDOR, solid state
curry	SQUID magnetometry
blochsteady	Bloch equations, steady-state
pulse	Shaped pulses
esfit	least-squares fitting

series of '.m' files that represent different abstractions of the overall modelling system that may or may not be implemented in the form of classes. For this thesis, we will use the term 'class' to refer to any modular component of the provided EasySpin library.

The most notable classes that are supplied with the library are the core plotting functions for ESR spectrums. These include such jocose names as "garlic" for cw isotropic ESR and "pepper" for solid state cw ESR (which we will use). Table 2.1 shows the full list of possible plotting functions supplied in the library. Other functions supplied in Easyspin are mostly related to data import/export, data analysis, and system optimizations.

In addition to the classes supplied in the EasySpin library, I have also built a few of my own for better visualization of spin systems. One such class (which is included in the online repository cited in the introduction) is called "zeeman.m". The purpose of this program is to draw the field splitting of the zeeman interactions in the spin system over increasing magnetic field. Another

Figure 2.3 The ESR spectrum presented by Stehr et al. for ZnO Nanowires at variable fields and angles.

class I implemented builds on top of this previous one and is called "animate.m". This will draw the zeeman diagram and then animate the plot by drawing the resonant magnetic field differences for given microwave frequency.

2.3 Selecting Hamiltonian Arguments

In addition to experimentally gathering the ESR data via ODMR, This thesis is also concerned with emulating the ESR spectrum via EasySpin. However, in order to do this the Hamiltonian for each material we will study needs to be understood to the best possible extent.

2.3.1 ZnO Nanowires

One of the works cited in this thesis investigates the resonant properties of zinc oxide nanowires. The author, Stehr, models the ESR spectrum using g-tensor and spin-values given for each defect center. This data is summarized in table 2.2. Stehr uses the *EasySpin* modeling system to show the predicted ESR spectrum resulting from the V_{Zn}^{-}, V_{Zn}/Zn_i, and D^* defect center contributions. He models each Hamiltonian separately using EasySpin and then combines the results with MATLAB. The figure 2.3 shows the plots that he presented to the journal after this process.

However, one thing Stehr did not include was the line-width parameters and derivations he used when constructing the spin system via EasySpin. As a verification for the process he used, I have included a reconstruction of the same ESR spectrum that was included in his paper. Through comparison I found that the line-width parameters used by Stehr were 1, 5, and 2 mT for V_{Zn}^{-}, V_{Zn}/Zn_i, and D^* respectively. Though it unknown as to how he arrived at these values, it is likely that he compared the theoretical model to the experimental data until a reasonable fit was achieved.

Table 2.2 Summary of the spin-Hamiltonian parameters for the various defect centers of ZnO nanowires given by J. E. Stehr et al. The spin-parity and diagonalized g-tensor values are given for each defect center. For the non-axial centers, φ is the angle between the z and c axis.

		Axial		Nonaxial			
Center	S	$g_\perp$	$g_\parallel$	g_{xx}	g_{yy}	g_{zz}	φ (deg)
V_{Zn}^-	$1/2$	2.0193	2.0024	2.0173	2.0183	2.0028	110.75
Z	$1/2$	2.006	2.020				20
V_{Zn}/Zn_i	1			1.9888	1.9893	1.9815	110.75
Zn_i^+	$1/2$	1.9595	1.9605				0
D^*	$1/2$	1.9595	1.9605				0

Figure 2.4 The recreation of the plots given by Stehr et al. for the ZnO nanowire ESR spectrum

In figure 2.4 I give the recreation of the spectrum in addition to the code used to generate the spin system that Stehr used.

2.3.2 Irradiated 4H-SiC

[Rough - More] One of the two primary materials studied in this thesis is silicon carbide. In order to compare the theoretical prediction for the ESR spectrum with experimental results we first need to discover what arguments are used in the overall spin Hamiltonian.

[Rough - More] SiC is a commonly known to be a spin-3/2 system with two major ESR peaks in its spectrum. The parameter âĂŸ.SâĂŹ given for the EasySpin system is then just $3/2$

[Rough - More] As mentioned previously, SiC has one major defect of interest: the silicon divacancy in its lattice structure. The g-factor for this defect center is given as ...

[Rough - More] The linewidths are relatively narrow for specimens related to SiC.

Figure 2.5 The representation of the known parameters included in the EasySpin struct definition for analysis of 4H-SiC

Figure 2.6 The representation of the known parameters included in the EasySpin struct definition for analysis of thin-film CdTe.

[Rough - More] One interesting property of this material is that it exhibits a zero-field splitting which divides the $+3/2$ and $+1/2$ from the $-1/2$ and $-3/2$ states even when there is no external magnetic field.

[Rough - More] Though it is not readily apparent, SiC also exhibits hyperfine splitting in its major ESR peaks.

[Rough - more] I have included the pertinent code to represent this system in terms of the aforementioned EasySpin struct definition in figure 2.5.

2.3.3 Thin-Film CdTe

[Rough - More] The other material of interest studied in this work is CdTe.

[Rough - more] This system exhibits a dominating Cd interstitial defect (I think. I should look that one up) which contributes a spin-1/2 term to the Hamiltonian.

[Rough - more] The crystal structure of CdTe is (IâĂŹll have to look this up) and thus the g-factor included in the Hamiltonian is (again, i have to look this up).

[Rough - more] I have included the pertinent code to represent this system in terms of the aforementioned EasySpin struct definition in figure 2.6.

Chapter 3

Experimental Methods

3.1 Preparation of Silicon Carbide Samples

3.2 Preparation of Cadmium Telluride Samples

3.3 Experiment Background

3.4 Experiment Setup

3.5 Data processing

Figure 3.1 This is the figure description.

Chapter 4

Results

4.1 Computational Predictions

4.2 Experimental Results

4.3 Data Analysis

4.4 Conclusion

Figure 4.1 This is the figure description.

Figure 4.2 This is the figure description.

Figure 4.3 This is the figure description.

Figure 4.4 This is the figure description.

Appendix A

Electron Spin Studies of Electron Irradiated SiC

Figure A.1 This is the figure description.

Figure A.2 This is the figure description.

Appendix B

Optical Studies of Cadmium Telluride

Figure B.1 This is the figure description..

Appendix C

Electron Spin Coherence of Silicon Vacancies in Proton-Irradiated 4H-SiC

word (Carlos et al. 2006) (Calusine et al. 2016) (Stoll 2015) (Stehr et al. 2013) (Stoll & Schweiger 2006) (Embley 2016) (Embley et al. 2017) (Miller 2015) (Poole 1967) (Muzafarova et al. 2016) (Stoll & Britt 2009) (Poole 1994) (Stavola 1998) (Kennedy & Glaser 1998) (Akhmedzhanov et al. 2016) (Shor 1999) (Bennett & Divincenzo 2000) (Baranov et al. 2011) (Srman et al. 2000) (Nehrkorn et al. 2015) (Bar-Gill et al. 2013) (Astakhov et al. 2016) (Carter et al. 2015) (Pake 1973) (**?**)

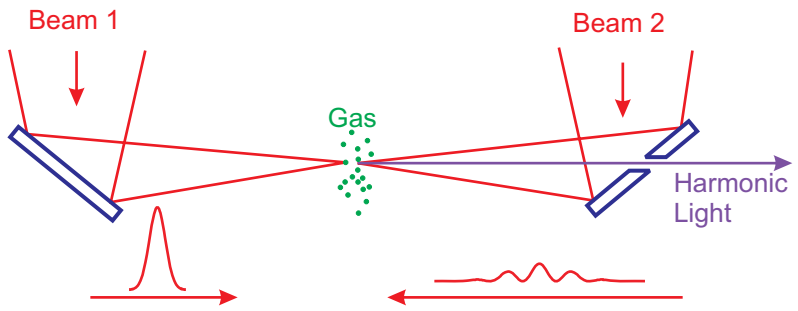

Figure 4.1 A mirror with a hole is used to extract high-order harmonics generated in counter-propagating laser beams.

Bibliography

Akhmedzhanov, R., Gushchin, L., Nizov, N., Nizov, V., Sobgayda, D., Zelensky, I., & Hemmer, P. 2016, Physical Review A - Atomic, Molecular, and Optical Physics, 94

Astakhov, G. V., et al. 2016, Applied Magnetic Resonance, 47, 793

Bar-Gill, N., Pham, L. M., Jarmola, A., Budker, D., & Walsworth, R. L. 2013, Nature Communications, 4

Baranov, P. G., Bundakova, A. P., Soltamova, A. A., Orlinskii, S. B., Borovykh, I. V., Zondervan, R., Verberk, R., & Schmidt, J. 2011, Physical Review B - Condensed Matter and Materials Physics, 83

Bennett, C. H., & Divincenzo, D. P. 2000, Nature, 404, 247

Calusine, G., Politi, A., & Awschalom, D. D. 2016, Physical Review Applied, 6

Carlos, W. E., Garces, N. Y., Glaser, E. R., & Fanton, M. A. 2006, Physical Review B - Condensed Matter and Materials Physics, 74

Carter, S. G., Soykal, O. O., Dev, P., Economou, S. E., & Glaser, E. R. 2015, Physical Review B - Condensed Matter and Materials Physics, 92

Embley, J. S. 2016, Electron Spin Coherence in Silicon Vacancy Defects of Proton-irradiated Silicon Carbide

Embley, J. S., et al. 2017, Electron spin coherence of silicon vacancies in proton-irradiated 4H-SiC

Kennedy, T. A., & Glaser, E. R. 1998, Magnetic Resonance of Epitaxial Layers Detected by Photoluminescence, Semiconductors and Semimetals, 93–136

Miller, K. G. 2015, Electron Spin Echo and Coherence Times in Silicon Carbide Defects

Muzafarova, M. V., Ilin, I. V., Anisimov, A. N., Mokhov, E. N., Soltamov, V. A., & Baranov, P. G. 2016, Physics of the Solid State, 58, 2406

Nehrkorn, J., Telser, J., Holldack, K., Stoll, S., & Schnegg, A. 2015, Journal of Physical Chemistry B, 119, 13816

Pake, G. E. 1973, The physical principles of electron paramagnetic resonance, 2nd edn. (W.A. Benjamin, Advanced Book Program, Reading, MA)

Poole, C. A. 1994, Handbook of electron spin resonance (American Institute of Physics, New York, N.Y.)

Poole, C. P. 1967, Electron spin resonance (Interscience Publishers, New York)

Shor, P. W. 1999, SIAM Review, 41, 303

Srman, E., Son, N. T., Chen, W. M., Kordina, O., Hallin, C., & Janzn, E. 2000, Physical Review B - Condensed Matter and Materials Physics, 61, 2613

Stavola, M. 1998, Identification of defects in semiconductors (Academic Press, San Diego)

Stehr, J. E., Chen, S. L., Filippov, S., Devika, M., Reddy, N. K., Tu, C. W., Chen, W. M., & Buyanova, I. A. 2013, Nanotechnology, 24, 015701

Stoll, S. 2015, Methods in Enzymology, Vol. 563, CW-EPR Spectral Simulations: Solid State

Stoll, S., & Britt, R. D. 2009, Physical Chemistry Chemical Physics, 11, 6614

Stoll, S., & Schweiger, A. 2006, Journal of Magnetic Resonance, 178, 42